

# **A GCM Parameterization of Bimodal Size Spectra for Ice Clouds**

*D. L. Mitchell and D. Ivanova  
Desert Research Institute  
Reno, Nevada*

*J. M. Edwards  
Hadley Centre for Climate Prediction and Research  
Meteorological Office  
Bracknell, United Kingdom*

*G. C. McFarquhar  
National Center for Atmospheric Research  
Boulder, Colorado*

## **Introduction**

The solar radiative properties of ice clouds are primarily a function of the ice water content (IWC) and the effective diameter (Mitchell et al. 1998a; Wyser and Yang 1998), defined as

$$D_{\text{eff}} = \text{IWC} / (\rho_i P_t), \quad (1)$$

where  $\rho_i$  = bulk ice density corresponding to refractive index measurements ( $0.92 \text{ g/m}^3$ ) and  $P_t$  = projected area of size distribution. However,  $D_{\text{eff}}$  cannot simply be measured in situ, but depends on ice crystal habit or shape, and the size distribution. An equation relating  $D_{\text{eff}}$  to ice particle shape and  $\bar{D}$ , the mean dimension (i.e., length) of a gamma size distribution,

$$N(D) = N_0 D^v \exp(-\lambda D), \quad (2)$$

is given in Mitchell et al. (1998a).

To date, the representation of  $D_{\text{eff}}$  for the ice phase in general circulation models (GCMs) has been highly uncertain, and is sometimes treated as constant or nearly constant. GCM sensitivity tests using the Hadley Centre's model indicate typical observed ranges of  $\bar{D}$  in ice clouds (e.g.,  $20 \mu\text{m}$  to  $400 \mu\text{m}$ ) leads to shortwave (SW) uncertainties of  $30 \text{ W m}^{-2}$  or more in cloudy regions. The aim of this work is to provide a means of estimating bimodal size spectra for ice clouds, which, with some informed assumption about ice particle shape, provides a means of estimating  $D_{\text{eff}}$  or radiative properties in general in GCMs.

## Tropical Cirrus

The main source of microphysical information for tropical cirrus to date consists of three anvil case studies from the Central Equatorial Pacific Experiment (CEPEX). Measured size spectra were shown to be bimodal (McFarquhar and Heymsfield 1996; 1997), with a minimum or shoulder near  $100 \mu\text{m}$ . This study uses the two-dimensional cloud (2DC) probe spectral data from all three case studies (March 17, April 1 and 4, 1993). While the 2DC provided usable information for  $D > 50 \mu\text{m}$ , where  $D$  = maximum ice particle dimension, the first two usable bins were in the small particle mode,  $N(D)_{\text{sm}}$ , of the bimodal distribution. Ice crystals having  $D < 50 \mu\text{m}$  were estimated from a log-linear line equation through these two bins, as illustrated in Figure 1, while the large particle mode,  $N(D)_{\text{l}}$ , was represented by another linear fit in log-linear space. This provided slope parameters  $\lambda_{\text{sm}}$  and  $\lambda_{\text{l}}$  for  $N(D)_{\text{sm}}$  and  $N(D)_{\text{l}}$ , respectively, where  $v = 0$ .

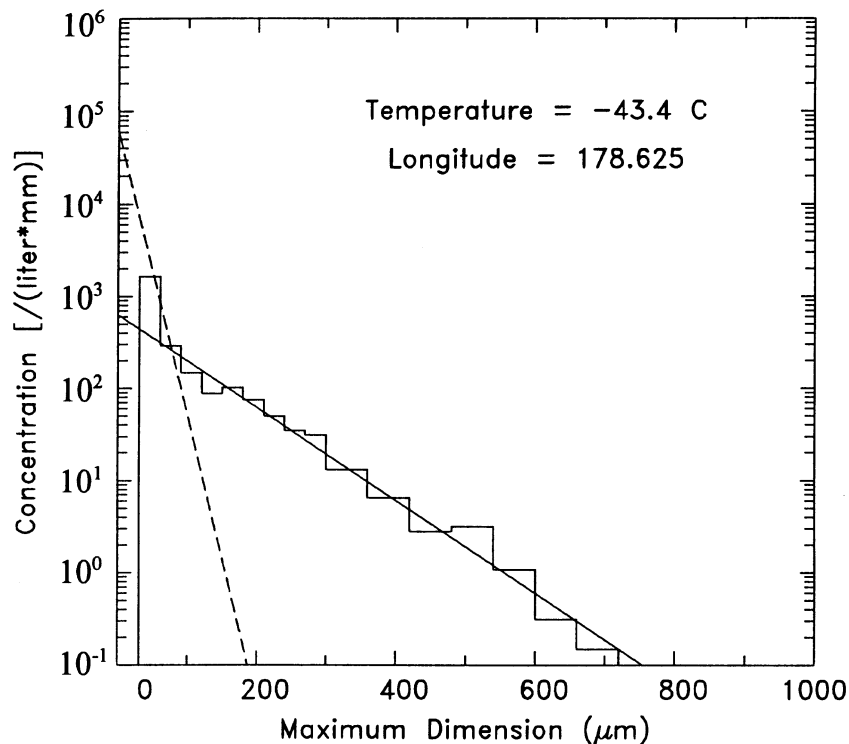


**Figure 1.** Example of a size distribution sampled during CEPEX, with linear fits describing the large and small ice particle modes.

The April 4 case study was a microphysics/radiation experiment, with the Modis Airborne Simulator (MAS) aboard the ER-2 measuring radiances in visible and near infrared channels. These radiances were simulated using an ice cloud radiation scheme (Mitchell et al. 1996), based on observed size spectra, the dominant observed crystal habit, and a Monte Carlo radiation transfer model (Macke et al. 1995). As described in Mitchell et al. (1998b), the first usable bin, known to be uncertain anyway, was

multiplied by a factor of 1.5 to yield optimal agreement with MAS radiances. This procedure generated the dashed line in Figure 1, and gave the estimated concentrations of undetected ice crystals for all three case studies. In this way, parameterized size spectra are known to yield the correct radiances as observed during the April 4 case study, assuming planar polycrystals with phase functions identical to hexagonal columns.

CEPEX size spectra were sampled in horizontal legs ranging from 150 km to 250 km at constant temperature (T), consisting of 19 usable legs in total. There were generally 5 to 6 spectra per leg, providing 93 “individual” values of  $\lambda$  and IWC. Individual  $\lambda$ s were averaged for each leg and these averages plotted against their corresponding temperature, as shown in Figure 2 for  $\lambda_1$ . Symbols refer to different case studies: March 17 = x, April 1 = o, April 4 = \*. Bars indicate standard deviations. Also shown for comparison is the  $\lambda$ -T relation for the reanalyzed Heymsfield-Platt data set (Platt 1997), obtained from mid-latitude cirrus. The  $\lambda$ -T relations for the CEPEX and mid-latitude cirrus are given, where T is in Celsius. Other measurements of size spectra in tropical cirrus are given in Knollenberg et al. (1993), where the tops of three tropical cyclones were sampled, and in Heymsfield (1986) for thin cirrus near the tropopause. These and the CEPEX data are combined in Figure 3. The three anvil tops in Knollenberg et al. had similar median mass dimensions,  $D_m$ , and are represented by a single value, “K”, in Figure 3 (after converting  $D_m$  to  $\bar{D}_1$ ). Note that  $\bar{D} = 1/\lambda$  for exponential spectra. The  $\bar{D}_1$ -T relation best representing these data is

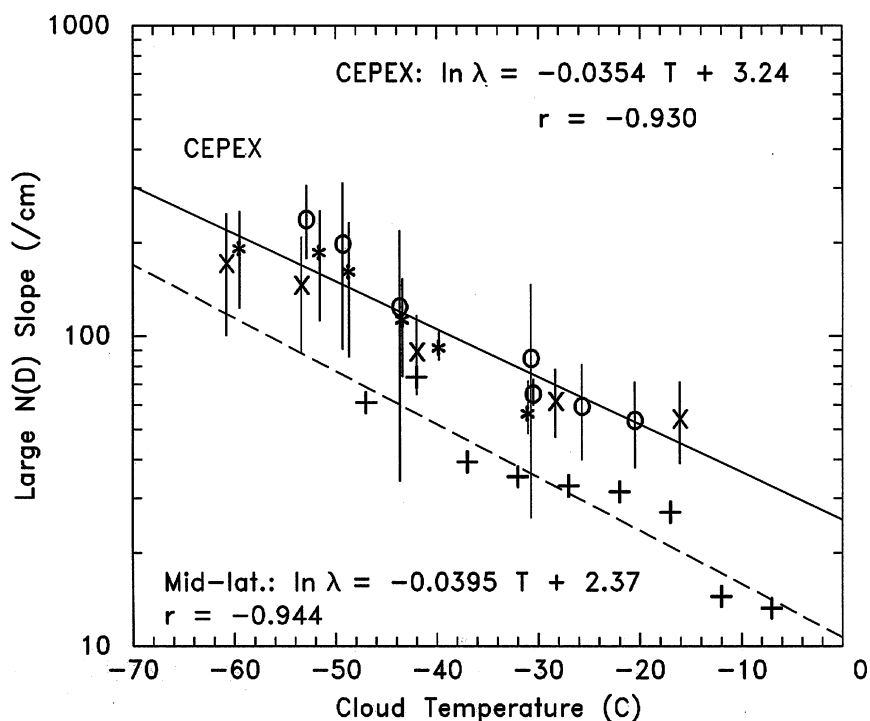


**Figure 2.** Correlation between large particle mode slope and temperature for the three CEPEX anvil clouds (March 17 = x, April 1 = o, April 4 = \*). The data (+) and linear fit described in Platt (1997) is shown for comparison.

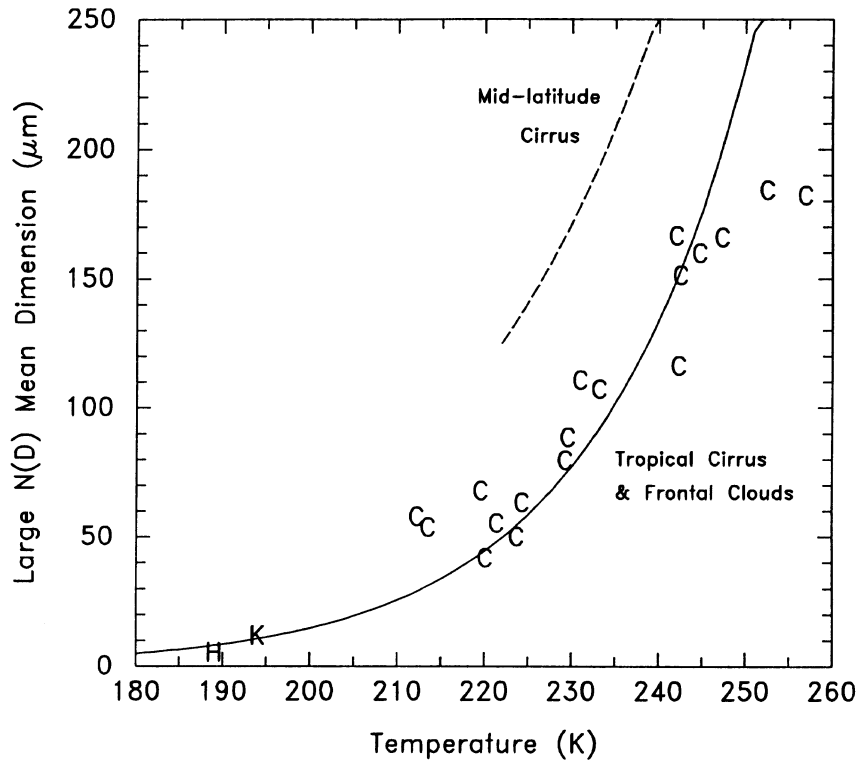


**Figure 3.** Temperature  $\bar{D}_1$  relation given by Eq. (3) for all tropical data (C=CEPEX, K=Knollenberg, H=Heymsfield) with the Platt (1997) relation (dashed curve) also given.

$$\bar{D}_1 = 1031 \exp [0.05522 (T - 277) ], \quad (3)$$

where  $\bar{D}_1$  is in  $\mu\text{m}$  and  $T$  is in degrees Kelvin. Some CEPEX data near cloud base (cloud top) show somewhat smaller (larger) sizes than predicted by Eq. (3). This may be due to sublimation (high condensation rates), which often characterize these two regions.

Next,  $\lambda_1$  and  $\lambda_{sm}$  are correlated in Figure 4, using the same symbols as in Figure 2 regarding case studies:

$$\lambda_{sm} = 1.49 \lambda_1 + 583, \quad (4)$$

where  $\lambda$  is in  $\text{cm}^{-1}$ . Uncertainty bars give standard deviations based on individual  $\lambda$  values at a given  $T$  level. While scatter among single  $\lambda$  values is considerable, much of this natural variability cancels when averaging over long horizontal legs, resulting in a correlation coefficient of 0.86. It is this mean behavior which is of relevance to GCMs.

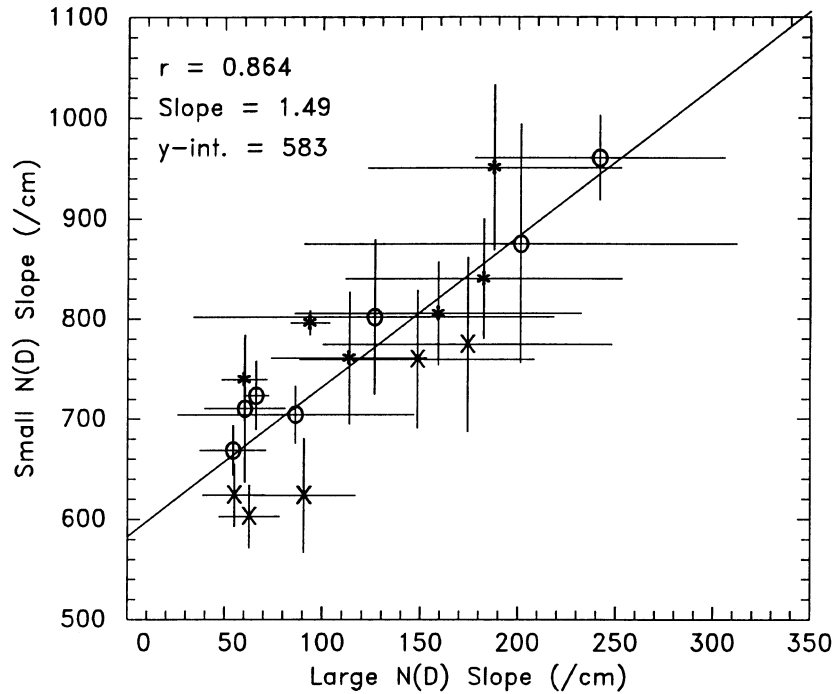


**Figure 4.** Correlation between the large and small particle mode slopes for the 3 CEPEX cases (symbols as before).

The last step in this parameterization is to partition the total IWC between  $N(D)_{sm}$  and  $N(D)_l$ , giving  $IWC_{sm}$  and  $IWC_l$ .  $IWC_{sm}$  was estimated from  $\lambda_{sm}$  and  $N_{o,sm}$  (y-intercept value corresponding to  $N(D)_{sm}$ ) as

$$IWC_{sm} = \alpha N_{o,sm} \Gamma(\beta+1) / \lambda_{sm}^{\beta+1}, \quad (5)$$

where  $\Gamma$  = gamma function, and the constants  $\alpha$  and  $\beta$  define ice particle mass  $m$  and depend on crystal habit:

$$m = \alpha D^\beta. \quad (6)$$

$IWC_l$  was determined by integrating over the size distribution, neglecting the first two bins. Planar polycrystals were assumed, although this is immaterial since no habit dependence occurs when ratioing these IWCs. The normalized IWCs (e.g.,  $IWC_l / (IWC_l + IWC_{sm})$ ) for the three case studies are plotted in Figure 5 as a function of  $\bar{D}_l$ . These values are not leg averages, but are for the individual spectra. It is seen that the partitioning of IWC between  $N(D)_l$  and  $N(D)_{sm}$  follows curves given by the relationship

$$IWC_{sm,n} = 0.025 [1 - \exp(-(\bar{D}_l / 80)^2)] + \exp(-(\bar{D}_l / 80)^2), \quad (7)$$

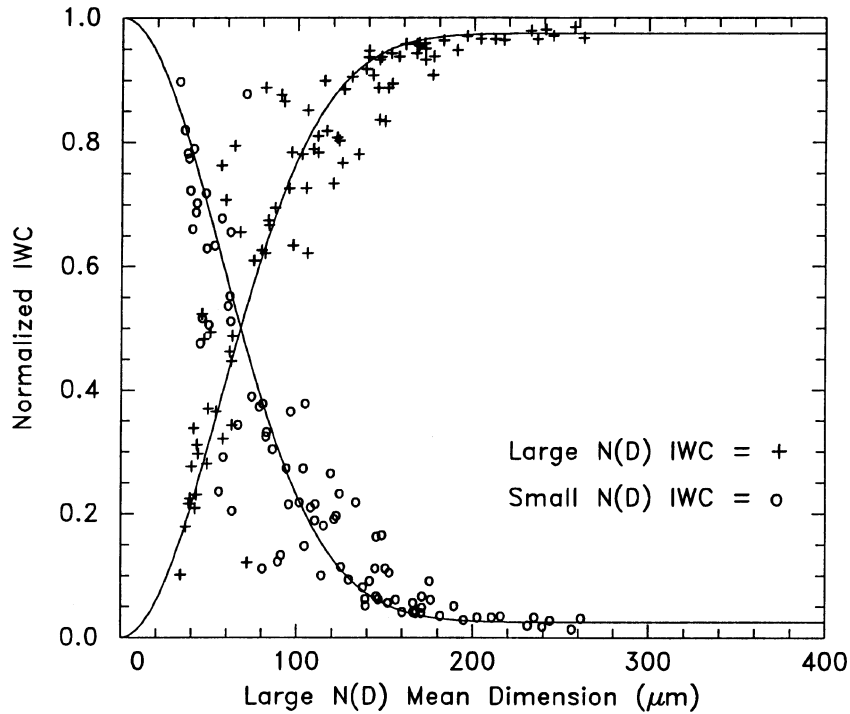


**Figure 5.** Partitioning of IWC between the small and large particle modes as a function of  $\bar{D}_1$  for the three CEPEX cases.

where  $IWC_{sm} = IWC_{sm,n} \times IWC_t$  and  $IWC_t$  is the total IWC given by a model.  $IWC_t$  is simply  $IWC_t - IWC_{sm}$ , and  $\bar{D}_1$  units =  $\mu\text{m}$ . Given the natural variability of measured size spectra, Eq. (7) appears to describe the partitioning of IWC fairly well.

Equations (3), (4), and (7) provide closure for estimating bimodal size spectra as a function of total IWC and temperature. Moreover,  $D_{\text{eff}}$  can be determined from Eq. (1) by noting  $P_t = P_{sm} + P_l$ , and that for exponential spectra,

$$P_x = \frac{\sigma_x \Gamma(\delta_x + 1)}{\alpha_x \Gamma(\beta_x + 1)} \frac{\beta_x - \delta_x}{IWC_x \lambda_x} \quad (8)$$

where x refers to either the “l” or “sm” subscript, and the projected area of an ice crystal is given as

$$P = \sigma D^\delta \quad (9)$$

where  $\sigma$ ,  $\delta$ ,  $\alpha$ , and  $\beta$  values for  $N(D)_{sm}$  and  $N(D)_l$  are given in Mitchell (1996). Alternatively, the radiation scheme of Mitchell et al. (1996) can be used, which directly uses  $\bar{D}_1$ ,  $\bar{D}_{sm}$ ,  $IWC_l$ , and  $IWC_{sm}$ , and is applicable in the thermal infrared as well (Mitchell et al. 1999).

## Frontal Clouds and Summary

In Ryan (1996),  $\lambda_1$  was related to T for ten field studies of winter mid-latitude frontal clouds in the northern and southern hemisphere, as shown in Figure 6. The thick solid line is our Eq. (3). It is seen that Eq. (3) is representative of the  $\lambda_1 - T$  relationships for frontal clouds. It is suggested that  $\lambda_1 - T$  relations may exhibit less “noise” when  $T < -15$  °C, since at warmer temperatures, ice multiplication effects can modify  $\lambda_1$  (see GM and AWSE in Figure 6), as well as enhanced aggregation rates due to dendrites (YL).

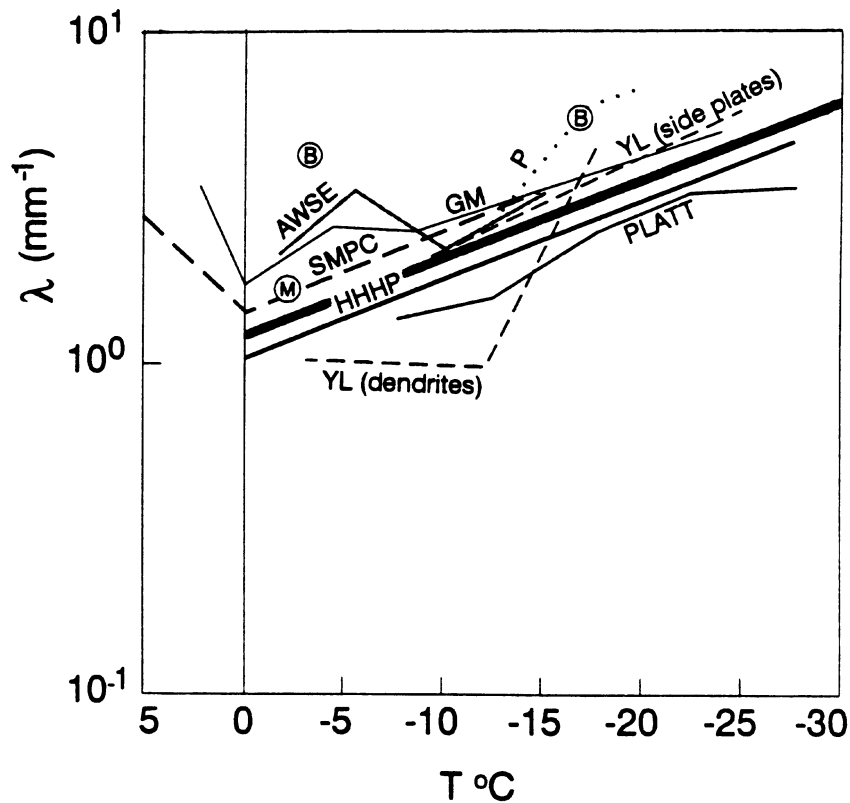


**Figure 6.** Temperature- $\lambda_1$  relations from frontal cloud field studies around the world, courtesy of B. Ryan (1996). Eq. (3) is given by the thick solid line.

At this time, it appears that Eqs. (3), (4), and (7) can be used to describe tropical cirrus clouds. For frontal clouds, Eq. (3) can probably be used, while for mid-latitude cirrus, the Platt (1997) relation might be substituted for Eq. (3). However, it is still unclear how the small crystal mode should be formulated for mid-latitude cirrus and ice in frontal clouds. Atmospheric Radiation Measurement (ARM) intensive observation period (IOP) data is currently being evaluated to develop a parameterization for these clouds. Additional microphysical and radiometric data are needed for all types of cirrus clouds to validate these findings and to determine whether, for a given T, significant differences in  $N(D)$  exist between tropical and mid-latitude cirrus.

## References

- Heymsfield, A. J., 1986: Ice particles observed in a cirriform cloud at  $-83^{\circ}\text{C}$  and implications for polar stratospheric clouds. *J. Atmos. Sci.*, **43**, 851-855.
- Knollenberg, R. G., K. Kelly, and J. C. Wilson, 1993: Measurements of high number densities of ice crystals in the tops of tropical cumulonimbus. *J. Geophys. Res.*, **98**, 8639-8664.
- Macke, A., Dlhopsky, J. Mueller, R. Stuhlmann, and E. Raschke, 1995: A study on bidirectional reflection functions for broken cloud fields over ocean. *Adv. Space Res.*, **16**, 50-58.
- McFarquhar, G. M., and A. J. Heymsfield, 1996: Microphysical characteristics of three anvils sampled during the Central Equatorial Pacific Experiment. *J. Atmos. Sci.*, **53**, 2401-2423.
- McFarquhar, G. M., and A. J. Heymsfield, 1997: Parameterization of tropical cirrus ice crystal size distributions and implications for radiative transfer: Results from CEPEX. *J. Atmos. Sci.*, **54**, 2187-2200.
- Mitchell, D. L., 1996: Use of mass- and area-dimensional power laws for determining precipitation particle terminal velocities. *J. Atmos. Sci.*, **53**, 1710-1723.
- Mitchell, D. L., W. P. Arnott, C. Schmitt, D. Lowenthal, and J. M. Edwards, 1999: Ice cloud absorption behavior in the thermal infrared inferred from laboratory extinction measurements. This proceedings.
- Mitchell, D. L., J. M. Edwards, and P. N. Francis, 1998a: GCM sensitivity of globally averaged albedo and OLR to ice crystal shape. In *Proceedings of the Seventh Atmospheric Radiation Measurement (ARM) Science Team Meeting*, CONF-970365. U.S. Department of Energy, Washington, D.C.
- Mitchell, D. L., A. Macke, and Y. Liu, 1996: Modeling cirrus clouds. Part II: Treatment of radiative properties. *J. Atmos. Sci.*, **53**, 2967-2988.
- Mitchell, D. L., G. M. McFarquhar, D. Ivanova, and A. Macke, 1998b: Testing an ice cloud radiation scheme with tropical anvil and mid-latitude case studies: Scattering implications. Preprints, Conf. on Light Scattering by Nonspherical Particles: Theory, Measurements and Applications. September 29-October 1, 1998, New York, New York.
- Platt, C.M.R., 1997: A parameterization of the visible extinction coefficient of ice clouds in terms of the ice/water content. *J. Atmos. Sci.*, **54**, 2083-2098.
- Ryan, B. F., 1996: On the global variation of precipitating layer clouds. *Bull. Amer. Meteor. Soc.*, **77**, 53-70.
- Wyser, K., and P. Yang, 1998: Average ice crystal size and bulk short-wave single-scattering properties of cirrus clouds. *Atmos. Res.*, **49**, 315-335.